A viscoelastic poromechanical model for shrinkage and creep of concrete

Abudushalamu Aili, Matthieu Vandamme, Jean-Michel Torrenti, Benoît Masson

Version of Record: https://www.sciencedirect.com/science/article/pii/S0008884619308178
Manuscript_87fe53db33dc501fee0d27b11c8d0aa0

A viscoelastic poromechanical model for shrinkage and creep of concrete

Abudushalamu Aili[a,*], Matthieu Vandamme[a,**], Jean-Michel Torrenti[b], Benoit Masson[c]

[a] *Laboratoire Navier, UMR 8205, École des Ponts ParisTech, IFSTTAR, CNRS, UPE, Champs-sur-Marne, France*
[b] *Université Paris-Est, IFSTTAR, 14 Boulevard Newton, F-77420 Champs-sur-Marne, France*
[c] *EDF Direction Technique DIPNN, Division CMG, groupe Génie Civil, 19 rue Pierre Bourdeix, F-69007, Lyon, France*

Abstract

Long-term delayed strain of concrete impacts the lifetime of civil engineering structures such as dams, nuclear power plants, nuclear waste storage tunnels or large bridges. In design practice, the long-term delayed strain of concrete is decomposed into four components: autogenous shrinkage, basic creep, drying shrinkage and drying creep. The four components are first computed separately and then summed up to obtain the total delayed strain of concrete, without wondering about any potential correlation between them. In this work, we aim at modeling the total delayed strain in a unified manner, without assuming this decomposition a priori. Such model is derived in the framework of viscoelastic poromechanics. The influence of relative humidity on the creep properties is taken into account. We assume that drying creep is due to the fact that the mechanical consequences of capillary effects are larger in loaded drying specimens than in non-loaded drying specimens. The model is validated by comparing the prediction with experimental results of delayed strain from the literature and discussed with respect to existing models.

Keywords: Concrete (E), Shrinkage (C), Creep (C), Humidity (A), Drying

*now at Graduate school of environmental studies, Naogoya University, Japan
**Corresponding author.
Email address: matthieu.vandamme@enpc.fr (Matthieu Vandamme)

(A)

1. Introduction

Long-term time-dependent strains of concrete are of great importance when it comes to analyze the security of major civil engineering concrete structures such as dams, nuclear power plants, nuclear waste storage tunnels or large bridges, as they are normally designed for a service lifetime of several decades. Conventionally, the delayed behavior of concrete is decomposed into autogenous shrinkage, basic creep, drying shrinkage and drying creep.

Autogenous shrinkage is the time-dependent strain of a non-loaded specimen exchanging no water with its surroundings. Many consider that autogenous shrinkage is caused by the capillary depression due to self-desiccation [1, 2, 3, 4, 5, 6, 7, 8, 9] while, recently, autogenous shrinkage was also attributed to eigenstresses that prevail in the solid skeleton as a result of hydration [10, 11, 12]. For what concerns the modeling of autogenous shrinkage as a response to capillary forces induced by self-desiccation, several authors [2, 4, 5, 8] considered autogenous shrinkage as an elastic response to those forces, while others [1, 3, 6, 7, 9, 13, 14, 15, 16, 17] considered it as a viscoelastic response to those same forces.

Basic creep is the difference between the strain of a loaded specimen exchanging no water with its surroundings and the autogenous shrinkage. Several theories exist in the literature to explain the physical origin of basic creep. For example, Bažant et al. [18] explained it with the microprestress theory, in which they postulated that, for load levels below 40% of the strength, the origin of the creep is the shear slip at overstressed creep sites. As a result of a progressive relaxation of microprestress at the creep sites and consecutive increase of their apparent viscosity, the creep rate observed under a constant applied stress declines over time. Recently, Vandamme [19] proposed, by joint analysis of results of macroscopic creep tests and microindentation creep tests, that basic creep originates from local microscopic relaxations.

Drying shrinkage is the difference between the strain of a non-loaded specimen exchanging water with its surroundings and the autogenous shrinkage. For cases where the relative humidity is larger than 40%, drying shrinkage is often considered to be caused by capillary effects. Again, some researchers [20, 21, 6, 14, 17] model drying shrinkage as the viscoelastic response of the material to those capillary effects while others (e.g., [22, 3, 23, 24, 25, 26]) consider it as an elastic response to those same forces.

Drying creep is the additional time-dependent strain of a loaded specimen exchanging water with its surroundings, with respect to the sum of autogenous shrinkage, basic creep and drying shrinkage. Drying creep is also known under the name of Pickett effect as it was observed first by Pickett [27]. The drying creep measured on a specimen can be divided into two parts: an intrinsic part and a part due to a structural effect. In a specimen in contact with dry air, drying takes place faster at the surface of the specimen than in its center, which hence creates a gradient of relative humidity through the specimen. In case of drying in absence of any mechanical load, the surface may crack, whereas cracking is limited by the load in case of drying under load. Hence, shrinkage in a cracking specimen should be less than in a non-cracking specimen (if it is possible to prevent a drying specimen from cracking) [28, 29]. When the specimen is loaded in compression, cracking is more limited and a supplementary part of the shrinkage is mobilized. This latter part of the strain is called drying creep related to the structural effect. The structural effect is not sufficient to explain the totality of drying creep [30, 29, 31]. The fraction of drying creep that cannot be explained by the structural effect is called the intrinsic drying creep, as it relates solely to the material. In the following, whenever drying creep is mentioned, we refer to its intrinsic part. The origin of (intrinsic) drying creep is still not known. Bažant et al. [32] consider that microdiffusion of water due to drying promotes shear slip in the microprestress theory [18], so that the kinetics of creep is faster in presence of drying than in absence of drying. This explanation is also supported by Vlahinic et al. [33] who propose that the migration of water molecules plays a lubricant role that amplifies delayed strain. Sinko et al. [34] propose that creep deformations are accelerated by the movement of water. In contrast, to explain drying creep, Sellier et al. [14] consider that the mechanical consequence of capillary forces applied to the solid skeleton is greater in presence of mechanical load than in absence of it.

Most design codes (e.g., Eurocode 2 [35], ACI [36] and code model [37]) and academic models in the literature [38, 39, 40, 41, 42, 43] follow such classical decomposition of delayed strains. In these models, each of the four components of delayed strain is computed individually with a different kinetic law. Then, by summing them up, the total delayed strain is obtained. However, with such approach, any potential correlation between the four components of delayed strain is not considered. For instance, drying creep and drying shrinkage are observed to be proportional to each other [44, 45]. In this work, we aim at proposing a predictive model that does not assume

this classical decomposition of delayed strains a priori.

From the origin of the four different components of delayed strains mentioned above, we can see that each of the four components can be considered to be a viscoelastic response to an applied external mechanical load or to internal capillary forces. Thus, in the spirit of the approach proposed by Sellier et al. [14], we could envision to model the various components of delayed strain in a unified manner, which will be attempted with poromechanics in the framework of non-aging isotropic linear viscoelasticity. By doing so, we aim at modeling the delayed strain of concrete without having to assume the classical decomposition a priori.

In this study, first, we list the main experimental tendencies that are to be taken into account in the model. The influence of relative humidity on both creep compliance and effective stress is discussed. Then, we present non-aging linear viscoelasticity with environment-dependent properties. Next, we estimate the elastic and long-term asymptotic values of the viscoelastic Biot coefficient, based on elastic and viscoelastic homogenization schemes. Then, the model is derived and calibrated against experimental results of delayed strain from the literature. In the end, the derived model is compared to other models from the literature and we list the advantages and weak points of the model and draw several conclusions.

2. Main lines of the model

Since, in this present work, we are mostly interested in the long-term delayed behavior of concrete (e.g., for containment buildings in nuclear power plants, where presetressing is applied when concrete is more than one-year-old), the model is dedicated to mature cementitious materials, for which we assume that the hydration slowed down significantly, that the microstructure does not change significantly anymore and that aging effect due to polymerization can be neglected [46, 47, 48]. Hence, the mechanical properties of the concrete are considered to be non-aging.

Up to about at least 40% of its strength, concrete behaves in a linear viscoelastic manner [49]. Therefore, the mechanical behavior of the concrete can be modeled in the framework of isotropic non-aging linear viscoelasticity: in isothermal conditions, the time-dependent state equations that link the stress tensor $\underline{\underline{\sigma}}$ (decomposed into the volumetric stress $\sigma_v = \mathrm{tr}(\underline{\underline{\sigma}})/3$ and the deviatoric stress tensor $\underline{\underline{s}}$ such that $\underline{\underline{\sigma}} = \sigma_v \underline{\underline{1}} + \underline{\underline{s}}$, where tr is the trace operator and $\underline{\underline{1}}$ is the unit tensor) to the strain tensor $\underline{\underline{\varepsilon}}$ (decomposed into

the volumetric strain $\varepsilon_v = \mathrm{tr}(\underline{\underline{\varepsilon}})$ and the deviatoric strain tensor $\underline{\underline{e}}$ such that $\underline{\underline{\varepsilon}} = (\varepsilon_v/3)\underline{\underline{1}} + \underline{\underline{e}}$) are [50]:

$$\varepsilon_v(t) = \int_{-\infty}^{t} J^K(t-\tau)\frac{\mathrm{d}\sigma_v(\tau)}{\mathrm{d}\tau}\mathrm{d}\tau \tag{1a}$$

$$e_{ij}(t) = \frac{1}{2}\int_{-\infty}^{t} J^G(t-\tau)\frac{\mathrm{d}s_{ij}(\tau)}{\mathrm{d}\tau}\mathrm{d}\tau \tag{1b}$$

where $t-\tau$ is the time since loading, and $J^K(t)$ and $J^G(t)$ are called the bulk creep compliance and the shear creep compliance, respectively. The bulk creep function, defined by $J^K(t) - J^K(0)$, is also widely used in the literature [51, 52, 53].

Water plays an important role in the delayed behavior of concrete, since concrete is subjected to capillary forces and surface forces related to the movement of pore fluid. Poromechanics [54] suits well to study the behavior of such a porous material.

We restrict the applicability of the model to relative humidities between 100% and 40%. In this range of relative humidity, mainly the water in capillary pores is affected [55]. Therefore, we consider in our model that concrete is composed of a solid skeleton and capillary pores. Partially saturated poromechanics [54], under the assumption of pore iso-deformation, states that the capillary stress σ_h due to a capillary pressure P_c reads (see Eq. (9.77) in [54]):

$$\sigma_h(t) = -\int_{-\infty}^{t} b(t-\tau)\frac{\mathrm{d}(S_l(\tau)P_c(\tau))}{\mathrm{d}\tau}\mathrm{d}\tau, \tag{2}$$

where b is the viscoelastic Biot coefficient, S_l is the saturation degree in liquid water and P_c is the capillary pressure. Then, under an applied external stress σ, the effective stress σ' that deforms the material reads:

$$\sigma' = \sigma + \sigma_h. \tag{3}$$

We want the model to capture the following experimental tendencies observed in the literature for the delayed behavior of concrete:

- Basic creep is observed to evolve as a logarithmic function of time in the long term for compressive stresses below 40% of the compressive

strength (see e.g., [56, 57] and data gathered in [58]), as supported also by nanoindentation [59] and microindentation creep experiments [53, 60]. Aili et al. [61] showed that the viscoelastic Poisson's ratio of concrete can be considered to be constant with respect to time and equal to 0.2. They also showed that the volumetric basic creep of concrete is non-asymptotic with time and evolves logarithmically with time at large times. Hence, we consider the following expression for the bulk creep compliance $J^K(t)$:

$$J^K(t) = \frac{1}{K} + \frac{1}{C^K}\log\left(1 + \frac{t}{\tilde{t}}\right), \tag{4}$$

where K is the (elastic) bulk modulus, C^K is the bulk creep modulus (which is defined, in a creep test performed under the stress σ_0, as the asymptotic value of $\sigma_0/(td\varepsilon/dt)$ in the long term [52]) and $\tilde{t}$ is a creep characteristic time. Combining this bulk creep compliance $J^K(t)$ with the assumption of a constant viscoelastic Poisson's ratio $\nu(t) = 0.2$, the three-dimensional viscoelastic behavior of concrete is fully described. Indeed, for a constant Poisson's ratio over time, the following relation is satisfied [62]:

$$J^G(t) = \frac{2(\nu+1)}{3(1-2\nu)}J^K(t). \tag{5}$$

where J^G is the shear creep compliance.

- Experimental observations [63, 64] showed that, under autogenous conditions, a pre-dried concrete creeps slower than a wet concrete. Therefore, the bulk creep modulus C^K in Eq. (4), which characterizes the long-term kinetics of creep, depends on the relative humidity h_r of the concrete:

$$C^K = C^K(h_r). \tag{6}$$

This dependence is also supported by results of microindentation tests [53, 60]. We identify this dependence in section 3. As for the characteristic time $\tilde{t}$ in Eq. (4), due to lack of experimental evidence, we assume it independent of relative humidity.

- Autogenous shrinkage is observed to evolve as a logarithmic function of time in the long term (see e.g., [16], based on data from the database gathered in [58]) for concretes with water-to-cement ratio lower than 0.5. This can be captured by considering autogenous shrinkage as creep under the action of capillary stress due to self-desiccation, as done in [1, 3, 6, 7, 9, 13, 14, 15, 16].

- Drying shrinkage is considered as the sum of the elastic and viscous responses of the material under the action of capillary forces due to desiccation, as done by others (e.g., [20, 21, 6, 14]).

- Drying creep, i.e., Pickett effect, manifests itself when drying occurs in the presence of a mechanical load. This part of the time-dependent strain will also be modeled as a viscoelastic strain, but the mechanical consequence of capillary forces will be considered to be larger in presence of a mechanical load than in absence of it, as done by Sellier et al. [14]. Such modeling will be performed by introducing a drying creep coefficient κ which is described in section 4.

3. Influence of relative humidity on creep modulus

In this section, we aim at modeling the dependence of the bulk creep compliance $J^K(t)$ on the relative humidity h_r (see Eq. 6). There is very few experimental data on the creep of predried specimens under autogenous conditions: [63, 64] by macroscopic testing and [53, 60] by microindentation testing. We use the microindentation results to infer the relation between bulk creep modulus C^K and relative humidity h_r.

The experimental microindentation results in [53, 60] provide the contact creep compliance $L(t)$, which is the inverse, in the Laplace domain, of the time-dependent indentation modulus $M(t)$. The contact creep modulus C^M is defined as the asymptotic value of $t(dL/dt) = (dL/d(\log(t))$ at large times.

Assuming the viscoelastic Poisson's ratio ν to be time-independent, the relation between contact creep modulus C^M and bulk creep modulus C^K is [59]:

$$C^K = \frac{1-\nu^2}{3(1-2\nu)} C^M, \tag{7}$$

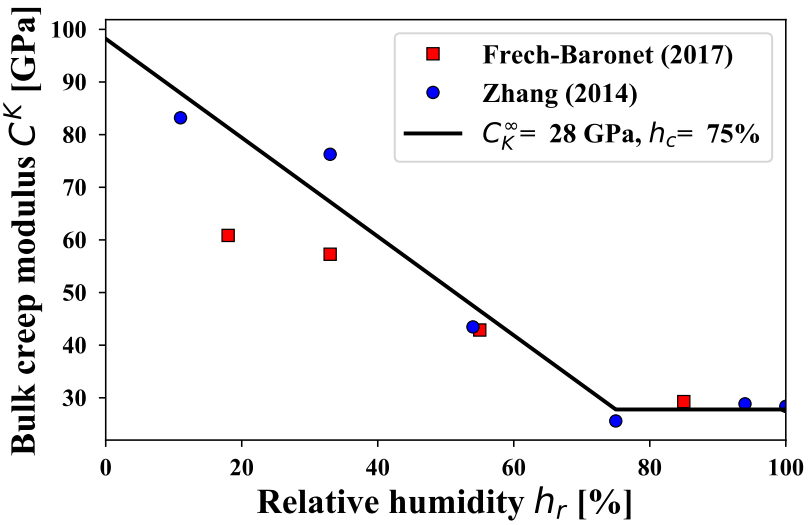

Figure 1: Bulk creep modulus of cement paste as a function of relative humidity obtained from the microindentation experiments in [53] and [60]

.

which makes it possible to infer, from microindentation data, the bulk creep modulus of cement paste as a function of relative humidity, which is plotted in Fig. 1. From the best fit of those results, this dependence is modeled as:

$$\frac{C^K(h_r)}{C^{K\infty}} = \begin{cases} 1 + \beta_{h_r}(h_c - h_r), & \text{if } h_r < h_c, \\ 1, & \text{if } h_r \geq h_c \end{cases} \tag{8}$$

where h_c=75%, $\beta_{h_r} = 3.35$ and $C^{K\infty}$ is the bulk creep modulus obtained by fitting basic creep of sealed sample.

4. Influence of relative humidity on effective stress

This section is dedicated to model the influence of relative humidity on the effective stress (see Eq. 3).

The capillary stress σ_h in Eq. (2) depends on relative humidity. On one hand, the saturation degree S_l is directly related to the relative humidity h_r via the desorption isotherm $S_l(h_r(t))$. On the other hand, the capillary pressure can be related to relative humidity through Kelvin's equation:

$$P_c = -\frac{RT}{V_w}\log(h_{r,K}), \tag{9}$$

where $R = 8.314\mathrm{J}\cdot\mathrm{K}^{-1}\cdot\mathrm{mol}^{-1}$, T and $V_w = 1.8\times10^{-5}\mathrm{m}^3/\mathrm{mol}$ are the ideal gas constant, the absolute temperature and the molar volume of water, respectively. $h_{r,K}$ captures the variations of relative humidity solely due to surface tension effects and to the curvature of the fluid/vapor menisci in the pore space. Noting the variations of relative humidity due to the presence of ions in the pore solution as $h_{r,S}$, the actual relative humidity h_r can be expressed as [65]:

$$h_r = h_{r,K}h_{r,S}. \tag{10}$$

Based on experimental data in [66, 67], Aili et al. [16] estimated in a previous study that the term $h_{r,S}$ is approximately equal to 0.97 in cement pastes under autogenous conditions. In this study, for the sake of simplicity, we neglect the effect of salts on the relative humidity. Said otherwise, we consider $h_{r,S} = 1$ or $h_r = h_{r,K}$.

The expression of effective stress in Eq. (3) also needs to capture the Pickett effect, i.e., drying creep. As mentioned in the introduction, there are presently mainly two types of explanation for the origin of drying creep. Correspondingly, there are presently mainly two ways to model the Pickett effect: 1) the variation $\dot{h_r}$ of relative humidity with respect to time in presence of an applied mechanical load is considered to impact the creep compliances $J^K(t)$ and $J^G(t)$, such as in the models in [32, 33]; 2) in a drying sample, the capillary stress σ_h transmitted to the solid skeleton in the presence of a compressive mechanical load is considered to be more important than in the absence of mechanical compressive load, such as in the model in [14]. In our present work, we choose the second way of modeling Picket effect, whereas the first way is discussed in section 9.1. To do so, we introduce a drying creep coefficient κ in the expression of the effective stress. In an incremental form, the effective stress σ'_v reads:

$$\mathrm{d}\sigma'_v = \mathrm{d}\sigma_v - \kappa\mathrm{d}\sigma_h. \tag{11}$$

When drying takes place in the absence of mechanical compressive load, we consider that κ is equal to 1. Said otherwise, the non-loaded drying condition is the reference state for the capillary stress (i.e., the condition in which we retrieve the classical expression of effective stress Eq. (3)). In contrast,

when drying takes place in presence of a compressive stress, κ is considered to be larger than 1. Said otherwise, σ_h is amplified by the compressive load. Hence, the drying creep coefficient κ is modeled as:

$$\kappa = \kappa(\sigma_v), \text{ with } \kappa(\sigma_v = 0) = 1. \tag{12}$$

For what concerns how the drying creep coefficient κ should vary with the load σ_v, it is difficult to conclude due to lack of experimental data. In design codes (e.g., code model [37]) and academic models in the literature (e.g., [38, 43]), the drying creep strain is supposed to be proportional to load, which implies here that the coefficient κ should be independent of the load. However, based on the hypothesis that the mechanical effect of the capillary stress is amplified in the presence of compressive stresses, one would rather expect a coefficient κ that varies with load level, which is in accordance with the model of Sellier et al. [14]. As a result, in a generic case and in absence of any further information, the drying creep coefficient κshould be considered to depend on load.

5. Non-aging linear viscoelasticity with environmental dependency

In this section, we aim at extending the constitutive equation (1) to the case where viscoelastic properties (i.e., compliances) depend on environmental parameters that are evolving with time. For the sake of simplicity, in this particular section we only consider a unidimensional case.

From the definition of compliance, the viscoelastic strain $\varepsilon(t, t_0)$ at time t under the application of a constant stress σ_0 that is applied since time t_0 is expressed as:

$$\varepsilon(t, t_0) = \sigma_0 J(t - t_0) \tag{13}$$

where $J(t - t_0)$ is the uniaxial creep compliance. If the stress $\sigma(t, t_0)$ applied since time t_0 varies over time, we can compute the strain response by using the principle of superposition, by decomposing the stress history either horizontally as shown in Fig. 2a, or vertically as shown in Fig. 2b. Walraven [68] showed that, when horizontal decomposition is used, the dependence on an environmental parameter $\mathbf{v}$ (e.g., temperature T in Fig. 2) cannot be taken into consideration. When the creep compliance depends on environmental parameters that evolve with time, we should instead use the vertical decomposition, as in Fig. 2b. Noting $J'(t, \mathbf{v}) = \partial J(t, \mathbf{v})/\partial t$, we relate the strain

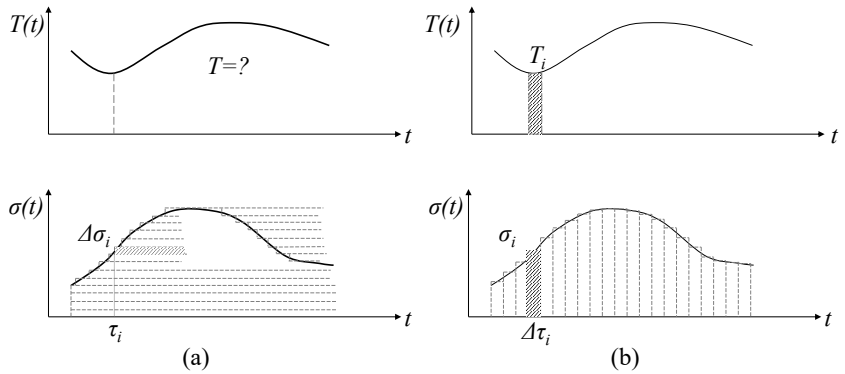

Figure 2: Principle of superposition by (a) horizontal decomposition of stress history and (b) vertical decomposition of stress history, taken from [68].

response to the stress history $\sigma(t, t_0)$ through:

$$\varepsilon(t, t_0) = \int_{-\infty}^{t} \sigma(\tau, t_0) J'(t - \tau, \mathbf{v}(\tau)) \mathrm{d}\tau, \tag{14}$$

where $\mathbf{v}$ is the environmental parameters on which the viscoelastic properties depend (for instance, temperature T in Fig. 2 or relative humidity h_r in our model). It is worth mentioning that the environment variable $\mathbf{v}$ in Eq. (14) should be evaluated at the same time as the load, which is consistent with [69]. The solution proposed by Shen and Walraven [68] to address problems with evolving environments seems intuitive and we used it here. However, it is not proven that this approach applies to all cases. If not, an alternative could be to assume that concrete behaves like a rheologically simple material [50]. This point will be the subject of further work.

6. Biot coefficient

While some properties of concrete such as creep compliance can be measured experimentally, the viscoelastic Biot coefficient is difficult to measure. Hence, in this section, we aim at estimating the viscoelastic Biot coefficient $b_c(t)$ of concrete through homogenization.

Concrete is a heterogeneous material made of various solid phases whose characteristic lengths vary from nanometers to centimeters. Based on the characteristic size of the various phases in microstructure of concrete, researchers [70, 71, 72, 73, 74, 75] proposed various multi-scale schemes for concrete, depending on the problem they wanted to resolve or on the method

of observation they used to characterize concrete. We follow the four-level multi-scale scheme presented in [61, 16] and displayed in Fig. 3. Then, using the expressions (Eqs. 20 and 24) of elastic Biot coefficient that are specified in [74], we estimate the elastic value b_c^0 and the long-term asymptotic value b_c^∞ of the viscoelastic Biot coefficient of the concrete. The steps of upscaling are the following:

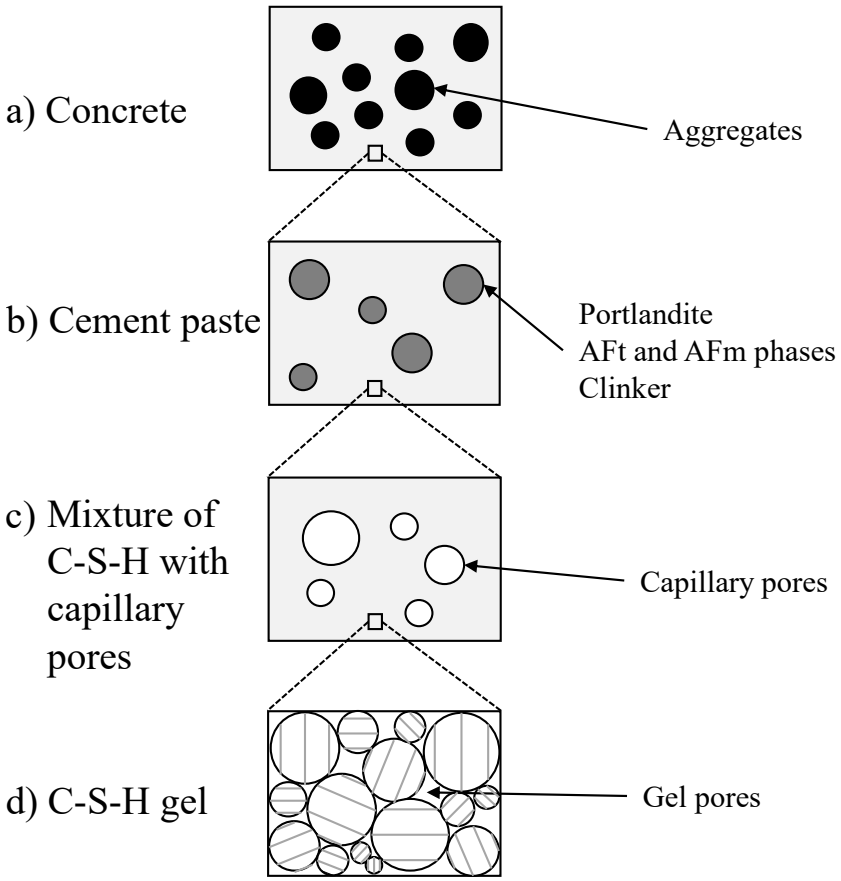

Figure 3: Multiscale structure of concrete: (a) Concrete as a matrix of cement paste embedding aggregates, (b) cement paste as portlandite, calcium sulfoaluminates hydrates and unhydrated clinker embedded into a matrix made of a mixture of C-S-H with capillary pores, (c) mixture of C-S-H with capillary pores as a matrix of C-S-H gel surrounding capillary porosity, and (d) C-S-H gel as a mixture of C-S-H particles and gel pores.

- At the finest scale (see Fig. 3d), the C-S-H gel is considered as a mixture of C-S-H particles and gel pores. We assume that C-S-H particles are

spherical and that the viscoelastic Poisson's ratio of the C-S-H gel is constant and equal to 0.2 [61]. Considering the self-consistent scheme, from Eq. (20) in [74], we obtain the elastic value b^0_{gel} of the viscoelastic Biot coefficient of the C-S-H gel:

$$b^0_{gel} = 2\phi_{gel}, \tag{15}$$

where ϕ_{gel} is the gel porosity, counted with respect to the volume of C-S-H gel. The long-term value b^∞_{gel} of the viscoelastic Biot coefficient is given, according to [16], by:

$$b^\infty_{gel} = 2\phi_{gel}, \tag{16}$$

which is equal to the elastic value.

- At a scale above (see Fig. 3c), the mixture of C-S-H gel with capillary pores is considered to be a matrix of C-S-H gel (which contains the gel porosity) that surrounds spherical capillary pores. Hence, the mixture of C-S-H gel with capillary pores is a two-scale porous material. Considering the Mori-Tanaka scheme, from Eq. (24) in [74] the elastic value b^0_{mix} of the viscoelastic Biot coefficient of the mixture of C-S-H gel with capillary pores reads:

$$b^0_{mix} = 1 - \frac{1-\phi_c}{1+\phi_c}(1 - b^0_{gel}), \tag{17}$$

where ϕ_c is the capillary porosity, counted with respect to the volume of the mixture of C-S-H gel with capillary pores. The long-term value b^∞_{mix} of the viscoelastic Biot coefficient at this scale is given, according to [16], by:

$$b^\infty_{mix} = 1 - \frac{1-\phi_c}{1+\phi_c}(1 - b^\infty_{gel}), \tag{18}$$

which is equal to the elastic value.

- Still at a scale above, i.e., at the scale of the cement paste (see Fig. 3b), portlandite, calcium sulfoaluminates hydrates and the unhydrated clinker are considered as spherical inclusions embedded into a porous matrix that is made of a mixture of C-S-H with capillary pores. Considering the Mori-Tanaka scheme, again from Eq. (24) in [74], the elastic value

b_p^0 of the viscoelastic Biot coefficient of the cement paste reads:

$$b_p^0 = 1 - f_{\mathrm{CH}} A_{\mathrm{CH}} - f_{\mathrm{alu}} A_{\mathrm{alu}} - f_{\mathrm{ck}} A_{\mathrm{ck}} - f_{mix} A_{mix}(1 - b_{mix}), \qquad (19)$$

where f_{CH}, f_{alu} and f_{ck} are the volume fractions of portlandite, calcium sulfoaluminate hydrates and unhydrated clinker with respect to the cement paste, respectively; A_{CH}, A_{alu}, A_{ck} are the spherical parts of the strain localization tensors of portlandite, calcium sulfoaluminate hydrates and unhydrated clinker, respectively. We consider that in the long term the inclusions deform much less than the matrix, i.e. that inclusions are much stiffer than the mixture of C-S-H gel with capillary pores. This results in $A_{\mathrm{CH}} \to 0$, $A_{\mathrm{alu}} \to 0$, $A_{\mathrm{ck}} \to 0$ and $A_{mix} \to 1/f_{mix}$. Inserting those limits into Eq. 19, the long-term value b_p^∞ of the viscoelastic Biot coefficient of the cement paste reads:

$$b_p^\infty = b_{mix}^\infty. \qquad (20)$$

- At the largest scale of concrete (see Fig. 3a), the aggregates are considered as spherical inclusions embedded into a porous matrix made of cement paste. Considering the Mori-Tanaka scheme, again from Eq. (24) in [74] the elastic value b_c^0 of the viscoelastic Biot coefficient of the concrete reads:

$$b_c^0 = 1 - f_p A_p (1 - b_p) - f_a A_a, \qquad (21)$$

where f_p and f_a are the volume fractions of cement paste and aggregate with respect to the volume of concrete, respectively; A_p and A_a are the spherical parts of the strain localization tensors of the cement paste and of the aggregates, respectively. We consider that in the long term the inclusions deform much less than the matrix, i.e. that the aggregates are much stiffer than the cement paste. This results in $A_a \to 0$ and $A_p \to 1/f_p$. Inserting those limits into Eq. 21, the long-term value b_c^∞ of the viscoelastic Biot coefficient of the concrete reads:

$$b_c^\infty = b_p^\infty. \qquad (22)$$

Combining Eqs. (15)-(22), we can estimate the elastic value b_c^0 and the long-term value b_c^∞ of the viscoelastic Biot coefficient of the concrete, based

Phase	Elastic bulk modulus [GPa]	Reference
C-S-H gel	15.6	Acker et el. (2001) [78], Constantinides and Ulm (2004) [71]
Portlandite	33.3	Constantinides and Ulm (2004) [71]
Calcium sulfoaluminates	33.3	Haecker et al. (2005) [79]
Unhydrated clinker	105.4	Boumiz et al. (1996) [80]

Table 1: Elastic bulk modulus of cement paste constituents from the literature.

on its water-to-cement ratio. The capillary porosity ϕ_c and gel porosity ϕ_{gel} can be estimated with Powers' model [76, 77] while the elastic bulk modulus of C-S-H gel, portlandite, calcium sulfoaluminate hydrates and unhydrated clinkers can be retrieved from the literature (see Tab. 1).

For what concerns the evolution over time of the viscoelastic Biot coefficient $b_c(t)$ of the concrete, similar to Eq. (9.28) in [22], we suppose an exponential evolution, as follows:

$$b_c(t) = b_c^{\infty} + (b_c^0 - b_c^{\infty}) \exp\left(-\frac{t}{\tilde{t}}\right). \tag{23}$$

Having no information on the characteristic time in the above Eq. (23), we simply take this characteristic time equal to the characteristic time $\tilde{t}$ (assumed independent of relative humidity) in Eq. (4). Since neither the elastic value nor the final value of the Biot coefficients depend on relative humidity (see Eqs. 15-22), the evolution over time of the Biot coefficient in Eq. 23 is independent of relative humidity. In spite of the assumption that the aggregates are much stiffer than the cement paste in the long term, it is worth mentioning that the long-term value of the Biot coefficient is not equal to 1, as a consequence of the multiscale heterogeneity of the solid skeleton. Indeed, because of this heterogeneity, the well-known elastic expression $b = 1 - K/K_s$ (where K_s is the bulk modulus of the solid skeleton) or its viscoelastic extension $b(t) = 1 - K(t) \odot J^{K_s}(t)$ [22] (where $K(t)$ is the bulk relaxation function of the porous solid, $J^{K_s}(t)$ is the bulk creep function of the solid skeleton, and $\odot$ holds for the Stieltjes convolution product) are not applicable to the material considered in this study, as those expressions are only valid for porous

materials with a homogenous solid skeleton.

7. Constitutive equations

In this section we list the procedure to model the time-dependent shrinkage and creep strains. We recall that the concrete/cement paste is considered as a non-aging viscoelastic porous material. We assume that the viscoelastic Poisson's ratio $\nu(t)$ is constant over time and equal to 0.2.

The model is a semi-coupled hydro-mechanical model: the relative humidity $h_r(t)$ affects the mechanical response $\underline{\underline{\varepsilon}}(t)$ but we neglect the impact of mechanical load on the history $h_r(t)$ of relative humidity (as this impact, which does exist [81], is rather small). Hence, the history $h_r(t)$ of relative humidity should be known, prior to any mechanical calculation. For the samples that are submitted to drying, the history $h_r(t)$ depends on the boundary conditions of the experiment and its determination may require solving a diffusion equation (e.g., [82, 42]). For the samples kept in autogenous conditions, we consider a constant relative humidity that is equal to the long-term relative humidity obtained in [16] by analyzing a set of 27 experiments from the literature:

$$h_r^{\infty}(w/c) = \begin{cases} 1 - 0.45(0.65 - w/c), & \text{if } w/c < 0.65, \\ 1, & \text{otherwise.} \end{cases} \tag{24}$$

The following material parameters and relations should be known in advance:

1. Bulk creep compliance $J^K(t)$ of the concrete or cement paste (depending on the sample that is tested), which can be obtained by measuring the elastic and basic creep strains.
2. Biot coefficient $b(t)$ of the concrete or cement paste, which, if not measured directly (as direct measurement is difficult), can be estimated through multi-scale homogenization (see section 6).
3. Creep modulus $C^K(t)$ of the concrete or cement paste, which depends on the relative humidity $h_r(t)$ and can be obtained with Eq. (8), since $C^{K\infty}$ is known from the bulk creep compliance $J^K(t)$.
4. Desorption isotherm $S_l(h_r)$ (or $S_l(P_c)$), which can be determined experimentally. We use Van Genuchten's law [83] to relate capillary pressure

P_c and saturation degree S_l:

$$P_c(S_l) = b_1 \left(S_l^{-\frac{1}{a_1}} - 1 \right)^{1-a_1}, \tag{25}$$

where a_1 and b_1 are material-specific Van Genuchten parameters which are dimensionless and expressed in Pascal, respectively. We can relate the capillary pressure P_c to the relative humidity h_r through Kelvin's law (Eq. 9). When no experimental measurement is available, desorption models available in the literature (e.g.,[84, 85, 86, 87, 88, 89, 90]) can be used.

Then, we compute the following state parameters step by step:

1. Water saturation degree $S_l(t)$ using the desorption isotherm;
2. Capillary pressure $P_c(t)$ using Kelvin's law (Eq. 9);
3. Capillary stress $\sigma_h(t)$ using Eq. (2);
4. Effective stress $\sigma'(t)$ by integrating Eq. (11);
5. Variation of bulk creep modulus $C^K(t)$ over time with Eq. (8);
6. Strain response $\underline{\underline{\varepsilon}}(t) = (\varepsilon_v/3)\underline{\underline{1}} + \underline{\underline{e}}$ using the following constitutive equations:

$$\varepsilon_v(t) = J^K(0)\sigma'_v(t) - \int_0^t \sigma'_v(\tau) J^{K'}(t-\tau, h_r(\tau))\mathrm{d}\tau \tag{26a}$$

$$e_{ij}(t) = J^G(0)s_{ij}(t) - \int_0^t s_{ij}(\tau) J^{G'}(t-\tau, h_r(\tau))\mathrm{d}\tau \tag{26b}$$

With such a model, the delayed strain of cement-based materials can be predicted in a unified manner.

For a non-loaded non-drying specimen, the strain response, which is equal to the autogenous shrinkage, is creep under the capillary stress due to self-desiccation. For a sufficiently mature specimen, this capillary stress is considered to have reached an asymptote, as the internal relative humidity does, leading to a long-term kinetics of autogenous shrinkage that is logarithmic with respect to time, as observed experimentally [16]. If the relative humidity remains equal to 100%, the delayed strain is 0.

For a loaded non-drying specimen, the strain response, which is equal to the sum of autogenous shrinkage and basic creep, is creep under a constant

stress that is equal to the sum of applied load and capillary stress. The basic creep evolves logarithmically over time in the long term.

For a non-loaded drying specimen, the strain response, which is equal to the sum of autogenous shrinkage and drying shrinkage, is creep under a capillary stress which evolves over time.

For a loaded drying specimen, the strain response, which is the sum of autogenous shrinkage, drying shrinkage, basic creep, and drying creep, is creep under a stress which is equal to the sum of the mechanically applied stress and of the capillary stress, and varies over time. The drying creep results from the assumption that the mechanical effect of the capillary stress that is transmitted to the solid skeleton is larger when the sample is under compressive load than when the sample is not loaded mechanically.

8. Application of model

In this section, we calibrate the model against experimental results from the literature. Since the model is intended for long-term delayed strain of mature concrete, we choose to consider the tests of Granger [40] and of the VeRCoRs project [91]. In both examples, we suppose that stresses and hydric state are homogeneous within each specimen.

8.1. Granger's experiments

Granger [40] studied the delayed behavior of six different concretes. The mix design of each of the six concretes corresponds to concretes used in the containment building of nuclear power stations. Excluding the concretes with silica fume, we focus ourselves on four of them: Flamanville, Chooz, Civaux B11, and Penly. The mix design properties of these concretes are given in Tab. 2.

For each of the concretes, Granger [40] measured the delayed strain under four different conditions: non-loaded non-drying condition, loaded non-drying condition, non-loaded drying condition and loaded drying condition. All specimens were kept sealed until the age of loading, i.e., 28 days. For the loaded specimen, an axial load of $\sigma_1 = 12$ MPa was applied instantaneously via a hydraulic pressure tank and kept constant afterwards. Drying started also at the time of loading under an ambient relative humidity of 50%. Beside the four tested specimens, another drying specimen was placed in the same room to measure mass loss over time.

Concrete	Water-to-cement ratio [-]	Saturated water content [m^3/m^3]	Estimated elastic Biot coefficient of concrete [-]	Estimated elastic Biot coefficient of cement paste [-]	Estimated long-term Biot coefficient of concrete [-]
Flamanville	0.48	0.106	0.32	0.72	0.82
Chooz	0.543	0.118	0.41	0.75	0.84
Civaux B11	0.557	0.129	0.46	0.76	0.85
Penly	0.577	0.133	0.43	0.77	0.86
VeRCoRs	0.52	0.072	0.33	0.74	0.79

Table 2: Properties of the concretes used in [40] and of concrete VeRCoRs [91]. Biot coefficients are estimated with Eqs. 15–22; the other parameters are from [40] and [91].

First, the Biot coefficient is estimated using Eqs. 15-22, resulting in the values listed in Tab. 2. In these estimations, elastic Biot coefficients at the scale of the cement paste are 0.72, 0.75, 0.76 and 0.77, respectively for the four types of concretes. Values are consistent with the estimation in [74]. Then, we compute the uniaxial creep compliance $J^E(t) = (1/E)+(1/C^E)\log\left(1+(t/\tilde{t})\right)$, where E is the uniaxial elastic modulus, C^E is the uniaxial creep modulus and $\tilde{t}$ is a characteristic time. The assumption of a time-independent viscoelastic Poisson's ratio equal to 0.2 makes it possible to compute the bulk $J^K(t)$ and shear $J^G(t)$ creep compliances. The results are listed in Tab. 3.

Then, combining the history of loss of mass over time with the water content at saturation given in Tab. 2, we obtain evolutions of saturation degree $S_l(t)$ over time. The history $P_c(t)$ of capillary pressure depends on the unknown Van Genuchten parameters a_1 and b_1 from Eq. (25). Based on the reported value of a_1 in the literature (e.g., [22, 92, 89, 14]) for ordinary concrete, we assume $a_1 = 0.5$. Kelvin's law (Eq. 9) provides then the history $h_r(t)$ of relative humidity. As a result, we obtain the capillary stress, which depends on the unknown Van Genuchten parameter b_1, and then, inserting the capillary stress in Eq. (11) and taking $\kappa = 1$, we obtain the effective stress σ'_v (which also depends on the unknown Van Genuchten parameter b_1) which acts on the non-loaded drying specimen. The dependence $C^K(t)$ of the bulk creep compliance on relative humidity is also taken into account based on the history $h_r(t)$ of relative humidity, using Eq. 8. Combining the effective stress

Concrete	E [GPa]	C^E [GPa]	$\tilde{t}^E$ [d]	a_1 [-]	b_1 [MPa]	$\kappa(\sigma = 12\text{MPa})$ [-]
Flamanville	22	94	15.5	0.5	20	1.8
Chooz	30	123	1.6	0.5	14	2.2
Civaux B11	29	125	2.5	0.5	13	2.8
Penly	31	173	1.1	0.5	14.2	1.8
VeRCoRs	30	126	44	0.44	19	1.7

Table 3: Parameters calibrated from experimental measurements of delayed strains. Experimental data are from [40]

.

with the creep compliance obtained from the basic creep strain (see Tab. 3) and inserting them into the viscoelastic stress-strain relation Eq. (26), we compute the strain of the non-loaded drying specimen. Finally, using the least-square method, we calibrate the value of the Van Genuchten parameter b_1 (see Tab. 3). The value of b_1 in the literature (e.g., [22, 92, 89, 14]) is reported to be in-between 30 and 60 MPa. Hence, the calibration of the model can be regarded as reasonable. The results of this calibration are displayed in Fig. 4.

The final step of the procedure is to calibrate the drying creep coefficient $\kappa(\sigma = 12\text{MPa})$, using the strain of the loaded drying specimen. For this specimen, knowing the capillary pressure P_c from Eq. (25), the effective stress σ'_v is computed from Eq. (11) as a function of the unknown drying creep coefficient $\kappa(\sigma = 12\text{MPa})$. Inserting this effective stress and humidity-dependent creep compliance into the viscoelastic relation (Eq. 26), we compute the strain of the loaded drying specimen as a function of the unknown drying creep coefficient $\kappa(\sigma = 12\text{MPa})$. Finally, using the least-square method, we calibrate the value of the coefficient $\kappa(\sigma = 12\text{MPa})$ (see Tab. 3). The results of this calibration are displayed in Fig. 4.

Instead of calibrating the drying creep coefficient κ in the last step, we could also assume a unique value $\kappa(\sigma = 12\text{MPa}) = 2$ for all mix designs and predict the strain of the loaded drying specimens. These prediction results are displayed with solid lines in Fig. 4 and compare relatively well with experimental measurements. From this prediction, we can see that, by considering a unique value for the coefficient $\kappa(\sigma = 12\text{MPa}) = 2$ for all concretes, we can predict reasonably well the drying creep and drying shrinkage. Therefore, setting $\kappa(\sigma = 12\text{MPa}) = 2$ seems to be a reasonable choice if all types of delayed strains have not been measured. Once the

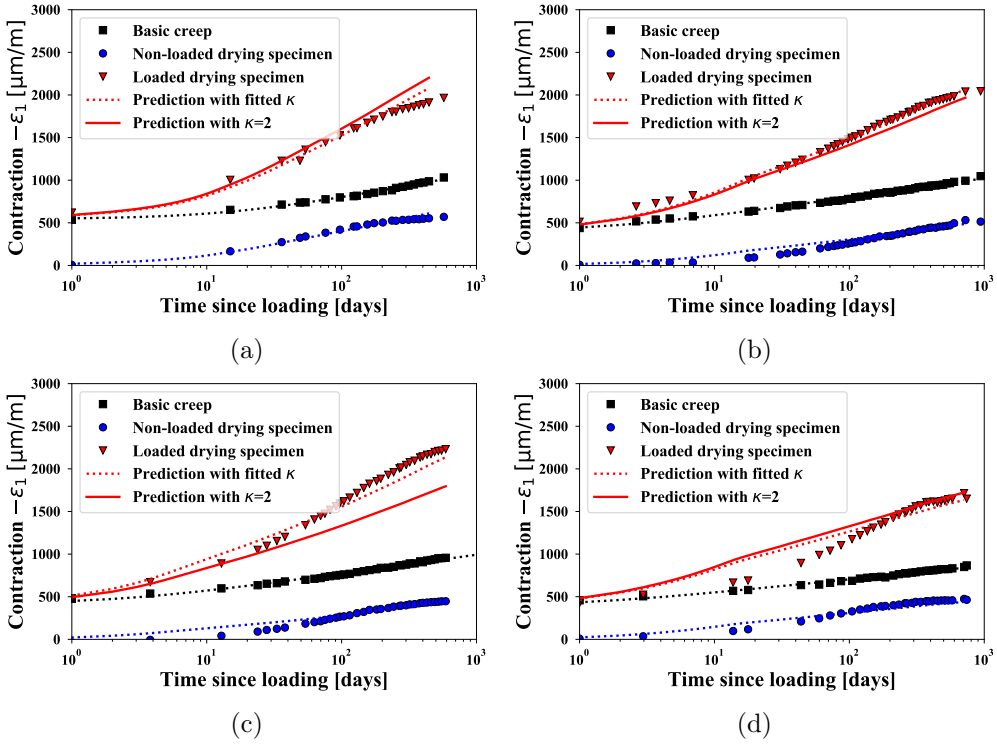

Figure 4: Calibration of the model against experimental measurement of delayed strain by [40]. Concretes correspond to the mixture of (a) Flamanville, (b) Chooz, (c) Civaux B11 and (d) Penly, respectively. Dashed lines are fitted; plain lines are prediction by assuming a drying creep coefficient κ=2. In (d), the dashed red line and solid red line overlap.

model is calibrated, we can predict the delayed strain under other hydric and loading conditions. In contrast, when all types of delayed strain tests are available, we can calibrate all parameters, i.e., drying creep coefficient κ included, from experimental results. The calibrated model can then be used to model the behavior of structures made with this specific concrete, eventually using numerical techniques such as finite elements.

8.2. Tests in VeRCoRs project

In the framework of the VeRCoRs project, [91, 93] characterized the delayed strains of the VeRCoRs concrete, whose water-to-cement ratio is equal to 0.52. The delayed strains were measured under four different conditions: non-loaded non-drying condition, loaded non-drying condition, non-loaded drying condition and loaded drying condition. All specimens were kept sealed

until the age of loading, i.e. 90 days. For the loaded specimen, an axial load of 12 MPa was applied instantaneously via a hydraulic pressure tank and kept constant afterward. Drying started also at the time of loading under an ambient relative humidity of 50%. The desorption isotherm was measured on other specimens made with the same concrete.

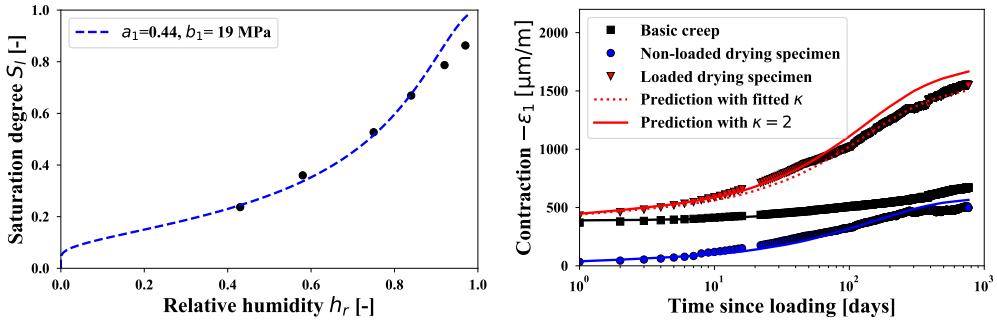

(a) (b)

Figure 5: (a) Desorption isotherm of VeRCoRs concrete; (b) Model calibration against experimental measurement of delayed strain on VeRCoRs concrete. Experimental data are from [91].

The first step of the model calibration is to compute the material parameters listed in section 7: the Biot coefficient is estimated using Eqs. 15-22 and listed in Tab. 2; the uniaxial creep compliance J^E is fitted against the measured strain and listed in Tab. 3. Again, the assumption of a time-independent viscoelastic Poisson's ratio equal to 0.2 makes it possible to compute the bulk $J^K(t)$ and shear $J^G(t)$ creep compliances. The Van Genuchten parameters a_1 and b_1 are fitted using the measured desorption isotherm.

Combining the desorption isotherm with the creep compliance, we can predict the delayed strain of the non-loaded drying specimen and of the loaded drying specimen. As for the loaded drying specimen, we can either calibrate the drying creep coefficient (the calibration yields $\kappa(\sigma = 12\text{MPa}) = 1.7$) or perform predictions by assuming that the drying creep coefficient is equal to $\kappa(\sigma = 12\text{MPa})=2$. The results are displayed in Fig. 5b, from which we can see that assuming $\kappa = 2$ gives a reasonable prediction of the strain of the loaded drying specimen. The comparison between the measured strains and predicted strains supports the idea that the four types of delayed strain can be modeled in a unified manner, as a viscoelastic strain resulting from the combined action of the applied mechanical load and/or of capillary stresses.

9. Discussion

In this section, we discuss the following three points: (1) alternative way of taking into account drying creep, (2) general comparison of the model here derived with existing models from the literature, (3) aspects to be considered in more details for improving the model.

9.1. Drying creep

As presented in the introduction, some researchers [18, 33] proposed that the moisture transport during drying promotes creep deformations. Therefore, instead of introducing a drying creep coefficient κ, an alternative way of modeling drying creep is to consider that the creep compliance is magnified when drying occurs. To do so in a simple way, we introduce a coefficient λ into the creep compliance in Eq. (4). The bulk creep compliance then reads:

$$\mathcal{J}^K(t) = \frac{1}{K} + \frac{\lambda}{C^K}\log\left(1 + \frac{t}{\tilde{t}}\right) \tag{27}$$

where:

$$\lambda = \lambda(\sigma_v, \dot{h_r}), \text{ with } \lambda(\sigma_v = 0 \text{ or } \dot{h_r} = 0) = 1. \tag{28}$$

Combining the creep compliance $\mathcal{J}^K(t)$ in Eq. (27) and the effective stress in Eq. (3) (without any drying creep coefficient), we can model the strain of a specimen under mechanical load or not, in combination with drying or not. For example, we can calibrate this alternative model on the experimental data of Granger [40] that are used in section 8.1. As a simple estimation, we consider that, upon drying, the non-zero coefficient λ is constant over time. The calibration is the same as the one performed in section 8.1, except for the last step, in which, using the strain response of the loaded drying specimen, instead of calibrating the drying creep coefficient, here we fit the parameter λ. The results of this calibration are presented in Fig. 6, where the best fit for parameter λ is 1.8, 1.7, 2.2, 1.5, respectively for Flamanville, Chooz, Civaux B11 and Penly. Similar to the analysis in section 8.1, we observe that a unique value of parameter $\lambda(\sigma = 12\text{MPa}, \dot{h_r} < 0) = 2$ predicts reasonably well the strain of the loaded drying specimen.

The model based on the coefficient λ provides roughly as good estimations as the model with drying creep coefficient κ, as seen by comparing Fig. 6 with Fig. 4. The mean values of the differences between measured and modeled values of strain on the loaded drying specimen are of comparable magnitude for the two methods. The differences at the last time step are

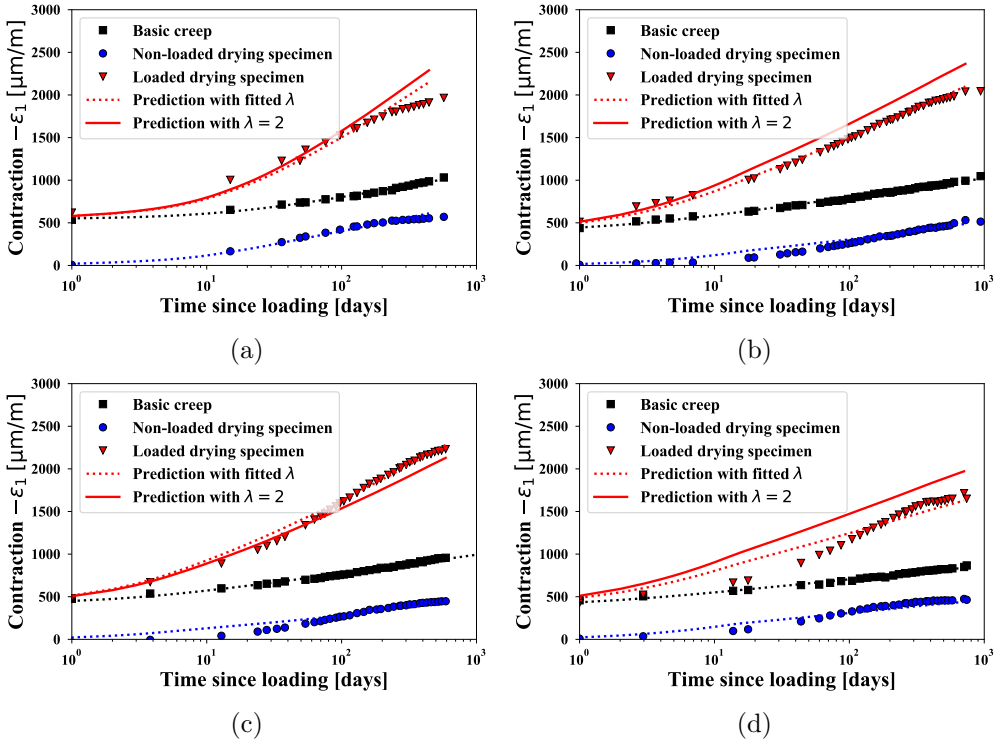

Figure 6: Calibration of the alternative model using Eq. (27) with coefficient λ against experimental measurement of delayed strain by [40]. Concretes correspond to the mixture of (a) Flamanville, (b) Chooz, (c) Civaux B11 and (d) Penly. Dashed lines are fitted, plain lines are prediction by assuming a coefficient λ=2.

also of comparable magnitude. Hence, it is difficult to suggest one method over the other one based on their accuracy.

In conclusion, drying creep can as well be captured by introducing a drying creep coefficient (see section 4) as by magnifying the creep compliances when drying occurs.

9.2. General comparison with existing models in literature

The model proposed in this work aims at modeling the long-term delayed strain of concrete without assuming the classical decomposition into autogenous/drying shrinkage and basic/drying creep, in the context of the evaluation of the long-term mechanical behavior of confinement buildings in French nuclear power plants. Hence, we used integral forms of the viscoelastic equations, i.e., creep compliances, which are used also in design codes

(e.g., Eurocode 2 [35], ACI [36] and code model [37]) and academic models in the literature [38, 39, 40, 41, 42, 43]. In contrast to the integral form, an incremental form of the equations is also widely used in academic models (e.g., [40, 42, 14]) as an incremental form makes it easier to implement the model in common finite element codes. All of these models, except the model of Sellier et al. [14], follow the classical decomposition of delayed strain into autogenous/drying shrinkage and drying/basic creep. In the following, we compare our model to the model of Sellier et al. [14].

Both Sellier et al.'s model [14] and our model are based on the theory of poromechanics. Though Sellier et al.'s model does not follow the classical decomposition of delayed strains, they decompose the strain into elastic, reversible time-dependent and irreversible time-dependent parts. An incremental form of the equations is used, based on rheological models. In contrast, our model uses one creep compliance which includes both elastic and time-dependent components. We did not consider the reversibility of strain. The fact that we use an integral form of the creep compliance is consistent with what is usually done in engineering practice. For what concerns the time-dependent behavior, the model of Sellier et al. [14] considers nonlinear viscoelasticity. Considering the fact that we targeted loads smaller than 40% of the strength, we restricted our model to linear viscoelasticity with respect to the applied load. The influence of relative humidity on the creep rate is considered in both models: Sellier et al. [14] take into account this influence by weighing the creep compliance with the saturation degree. In our model, we consider the dependency of the creep modulus on relative humidity, based on microindentation tests from the literature. In both models, the capillarity-induced stress that is transmitted to the solid skeleton is considered to be larger when the drying specimen is loaded than when it is not loaded, which makes it possible to take into account drying creep (i.e. Pickett effect). Sellier et al. [14] used a constant Biot coefficient which is equal to the Biot coefficient at saturated state. In contrast, in our model, the time dependence of the viscoelastic Biot coefficient is recognized: in the framework of our model, recognizing this time dependence is necessary to predict delayed strains accurately. Moreover, we showed in section 9.1 that, in our model, we can easily integrate an alternative explanation of drying creep, according to which drying creep originates from an increase of creep compliance due to water migration during drying.

9.3. Points to improve

The model could be enriched by considering in more details the following aspects:

- Firstly, the structural effect of drying is not considered in the model: the model is only formulated at material level. The gradient of relative humidity due to an inhomogeneous drying causes tensile stresses in the skin of the concrete. As a result, damage occurs when the tensile stresses are higher than the tensile strength of concrete; consequently, the effective section decreases. [29, 31, 42] showed that a significant fraction of drying creep is related to this structural effect. Incorporating this structural effect into the analysis of the experiments used in section 8 would be beneficial to better predict the strain behavior of a drying concrete specimen. This could be achieved by implementing the model in a finite-element code and coupling it with a computation of the desiccation of concrete and eventually with cracking models. It should be noticed that to compute strain increment at each time step in a finite element code, the model requires access to parameters from all of the previous steps. To implement the model in an existing finite element code for which such access is not possible, one may approximate the logarithmic creep compliance with a chain of Kelvin-Voigt elements [94] and write down the model in an incremental form.

- Secondly, as mentioned in section 4, considering that the drying creep coefficient κ is constant over time is questionable. Since this parameter κ is intended to characterize the influence of the applied mechanical load on how capillary stresses are transmitted to the solid skeleton during drying, the magnitude of the parameter κ should be related to the intensity of this drying. Said otherwise, one could expect that the drying coefficient κ would vary over time, because of the desiccation varying over time. Numerical simulations of concrete drying could provide some information about how this parameter κ varies over time and space during the drying.

- Drying creep could be modeled in two alternative manners: 1) by introducing a drying creep coefficient (see section 4) or 2) by modifying the magnitude of the long-term creep by introducing a coefficient λ (see section 9.1). With both models, capturing drying creep requires

the introduction of a parameter that is somewhat phenomenological, which is not fully satisfactory given our ambition of providing a unified poromechanical model with a sound physical basis. The need for introducing such phenomenological parameter can be due to the fact that the physical origin of drying creep is still not fully clear (see e.g., [33, 95]).

10. Conclusions

In this work, we proposed a non-aging linear viscoelastic poromechanical model to predict the delayed strain of cement-based materials, without decomposing the delayed strain classically into autogenous/drying shrinkage and basic/drying creep. The model is dedicated to delayed strains of mature materials, i.e., materials whose microstructure does not change significantly with time anymore. Consequently, the model cannot simulate shrinkage and creep behavior related to or caused by hydration at early age. For what concerns the load range, the model is only applicable to cases where the applied load does not exceed 40% of the strength. Several conclusions can be drawn:

- The delayed strains of concrete under various mechanical and hydric conditions could be predicted with a non-aging linear viscoelastic poromechanical model, without assuming the classical decomposition used in the literature or in design codes, which considers the total delayed strain to be the sum of autogenous/drying shrinkage and basic/drying creep.

- To capture drying creep (i.e. Picket effect), we needed to introduce a drying creep coefficient (see section 4) or, alternatively, a parameter to modify the creep compliance (see section 9.1). Considering a drying creep coefficient $\kappa(\sigma = 12\text{MPa})=2$ provided reasonably good predictions of the delayed strains of a loaded drying specimen, for all mix designs considered.

Acknowledgments

The authors acknowledge financial support from EDF and thank EDF for this support.

References

[1] C. Hua, P. Acker, A. Ehrlacher, Analyses and models of the autogenous shrinkage of hardening cement paste: I. modelling at macroscopic scale, Cement and Concrete Research 25 (7) (1995) 1457–1468.

[2] P. Lura, O. M. Jensen, K. van Breugel, Autogenous shrinkage in high-performance cement paste: an evaluation of basic mechanisms, Cement and Concrete Research 33 (2) (2003) 223–232.

[3] D. Gawin, F. Pesavento, B. A. Schrefler, Hygro-thermo-chemo-mechanical modelling of concrete at early ages and beyond. part ii: shrinkage and creep of concrete, International Journal for Numerical Methods in Engineering 67 (3) (2006) 332–363.

[4] F. Lin, C. Meyer, Modeling shrinkage of portland cement paste, ACI materials journal 105 (3) (2008) 302–311.

[5] L. Stefan, F. Benboudjema, J.-M. Torrenti, B. Bissonnette, Behavior of concrete at early stage using percolation and biot's theory, in: Proceedings of the 4th Biot conference on Poromechanics, 2009.

[6] Z. C. Grasley, C. K. Leung, Desiccation shrinkage of cementitious materials as an aging, poroviscoelastic response, Cement and Concrete Research 41 (1) (2011) 77–89.

[7] M. Wyrzykowski, P. Lura, F. Pesavento, D. Gawin, Modeling of internal curing in maturing mortar, Cement and Concrete Research 41 (12) (2011) 1349–1356.

[8] J. Zhang, D. Hou, Y. Han, Micromechanical modeling on autogenous and drying shrinkages of concrete, Construction and Building Materials 29 (2012) 230–240.

[9] Y. Luan, T. Ishida, C.-H. Li, Y. Fujikura, H. Oshita, T. I. T. Nawa, T. Sagawa, Enhanced shrinkage model based on early age hydration and moisture status in pore structure, Journal of Advanced Concrete Technology 11 (12) (2013) 1–13.

[10] F.-J. Ulm, R. J. Pellenq, Shrinkage due to colloidal force interactions, in: CONCREEP 10, 2015, pp. 13–16.

[11] M. Abuhaikal, Expansion and shrinkage of early age cementitious materials under saturated conditions: the role of colloidal eigenstresses, Ph.D. thesis, Massachusetts Institute of Technology (2016).

[12] M. Abuhaikal, K. Ioannidou, T. Petersen, R. J.-M. Pellenq, F.-J. Ulm, Le châteliers conjecture: Measurement of colloidal eigenstresses in chemically reactive materials, Journal of the Mechanics and Physics of Solids 112 (2018) 334–344.

[13] A. Hajibabaee, Z. Grasley, M. Ley, Mechanisms of dimensional instability caused by differential drying in wet cured cement paste, Cement and Concrete Research 79 (2016) 151–158.

[14] A. Sellier, S. Multon, L. Buffo-Lacarrière, T. Vidal, X. Bourbon, G. Camps, Concrete creep modelling for structural applications: non-linearity, multi-axiality, hydration, temperature and drying effects, Cement and Concrete Research 79 (2016) 301–315.

[15] X. Li, Z. C. Grasley, J. W. Bullard, E. J. Garboczi, Irreversible desiccation shrinkage of cement paste caused by cement grain dissolution and hydrate precipitation, Materials and Structures 50 (2) (2017) 104.

[16] A. Aili, M. Vandamme, J.-M. Torrenti, B. Masson, Is long-term autogenous shrinkage a creep phenomenon induced by capillary effects due to self-desiccation?, Cement and concrete research 108 (2018) 186–200.

[17] S. Rahimi-Aghdam, E. Masoero, M. Rasoolinejad, Z. P. Bažant, Century-long expansion of hydrating cement counteracting concrete shrinkage due to humidity drop from selfdesiccation or external drying, Materials and Structures 52 (1) (2019) 11.

[18] Z. P. Bažant, A. B. Hauggaard, S. Baweja, F.-J. Ulm, Microprestress-solidification theory for concrete creep. i: Aging and drying effects, Journal of Engineering Mechanics 123 (11) (1997) 1188–1194.

[19] M. Vandamme, Two models based on local microscopic relaxations to explain long-term basic creep of concrete, Proceedings of the Royal Society A 474 (2220) (2018) 20180477.

[20] F. Benboudjema, F. Meftah, J.-M. Torrenti, A viscoelastic approach for the assessment of the drying shrinkage behaviour of cementitious materials, Materials and Structures 40 (2) (2007) 163–174.

[21] A. Sellier, L. Buffo-Lacarriere, Towards a simple and unified modelling of basic creep, shrinckage and drying creep of concrete, European Journal of Environmental and Civil Engineering 13 (10) (2009) 1161–1182.

[22] O. Coussy, Poromechanics, John Wiley & Sons, 2004.

[23] I. Maruyama, Origin of drying shrinkage of hardened cement paste: hydration pressure, Journal of Advanced Concrete Technology 8 (2) (2010) 187–200.

[24] M. B. Pinson, E. Masoero, P. A. Bonnaud, H. Manzano, Q. Ji, S. Yip, J. J. Thomas, M. Z. Bažant, K. J. Van Vliet, H. M. Jennings, Hysteresis from multiscale porosity: modeling water sorption and shrinkage in cement paste, Physical Review Applied 3 (6) (2015) 064009.

[25] C. Di Bella, M. Wyrzykowski, P. Lura, Evaluation of the ultimate drying shrinkage of cement-based mortars with poroelastic models, Materials and Structures 50 (1) (2017) 52.

[26] M. Rezvani, T. Proske, C.-A. Graubner, Modelling the drying shrinkage of concrete made with limestone-rich cements, Cement and Concrete Research 115 (2019) 160–175.

[27] G. Pickett, The effect of change in moisture-content on the creep of concrete under a sustained load, in: Journal Proceedings, Vol. 38, 1942, pp. 333–356.

[28] P. Acker, Comportement mécanique du béton: apports de l'approche physico-chimique, no. 152, Rapport de recherche des LPC (in French), 1988.

[29] Z. P. Bažant, Y. Xi, Drying creep of concrete: constitutive model and new experiments separating its mechanisms, Materials and structures 27 (1) (1994) 3–14.

[30] Z. P. Bažant, J.-C. Chern, Stress-induced thermal and shrinkage strains in concrete, Journal of Engineering Mechanics 113 (10) (1987) 1493–1511.

[31] L. Granger, J.-M. Torrenti, P. Acker, Thoughts about drying shrinkage: experimental results and quantification of structural drying creep, Materials and structures 30 (10) (1997) 588.

[32] Z. Bažant, J. Chern, Concrete creep at variable humidity: constitutive law and mechanism, Materials and structures 18 (1) (1985) 1–20.

[33] I. Vlahinić, J. J. Thomas, H. M. Jennings, J. E. Andrade, Transient creep effects and the lubricating power of water in materials ranging from paper to concrete and kevlar, Journal of the Mechanics and Physics of Solids 60 (7) (2012) 1350–1362.

[34] R. Sinko, M. Vandamme, Z. P. Bažant, S. Keten, Transient effects of drying creep in nanoporous solids: understanding the effects of nanoscale energy barriers, Proceedings of the Royal Society A: Mathematical, Physical and Engineering Sciences 472 (2191) (2016) 20160490. doi:10.1098/rspa.2016.0490.

[35] E. 1992-1-1:2005, Eurocode 2: Design of Concrete Structures: Part 1-1: General Rules and Rules for Buildings, CEN, 2004.

[36] ACI Committee 209, Guide for Modeling and Calculating Shrinkage and Creep in Hardened Concrete (ACI 209.2R-08), American Concrete Institute, 2008.

[37] FIB, Model code for concrete structures 2010, Ernst and Son.

[38] RILEM Technical Committee, Creep and shrinkage prediction model for analysis and design of concrete structures-model b3, Materials and Structures 28 (1995) 357–365.

[39] R. Le Roy, Déformations instantanées et différées des bétons à hautes performances, Ph.D. thesis, École Nationale des Ponts et Chaussées (1995).

[40] L. Granger, Comportement différé du béton dans les enceintes de centrales nucléaires: analyse et modélisation, Ph.D. thesis, Ecole Nationale des Ponts et Chaussées (1995).

[41] N. Gardner, M. Lockman, Design provisions for drying shrinkage and creep of normal-strength concrete, Materials journal 98 (2) (2001) 159–167.

[42] F. Benboudjema, F. Meftah, J.-M. Torrenti, Interaction between drying, shrinkage, creep and cracking phenomena in concrete, Engineering structures 27 (2) (2005) 239–250.

[43] RILEM Technical Committee, RILEM draft recommendation: TC-242-MDC multi-decade creep and shrinkage of concrete: material model and structural analysis, Materials and Structures 48 (4) (2015) 753–770. doi:10.1617/s11527-014-0485-2.

[44] B. Gamble, L. Parrott, Creep of concrete in compression during drying and wetting, Magazine of concrete research 30 (104) (1978) 129–138.

[45] R. Le Roy, F. De Larrard, P. Gérard, Calcul des déformations instantanées et différées des bétons hautes performances, Bulletin des laboratoires des Ponts et Chaussées Spécial XIX (1998) 63–84.

[46] Z. Bažant, Material models for structural creep analysis. mathematical modeling of creep and shrinkage of concrete, ed. zp bazănt (1988).

[47] Z. Wang, Y. Han, Y. Hua, Research on increasing effect of solution polymerization for cement-based composite, Cement and Concrete Research 33 (10) (2003) 1655 – 1658. doi:https://doi.org/10.1016/S0008-8846(03)00140-6.
URL http://www.sciencedirect.com/science/article/pii/S0008884603001406

[48] H. M. Jennings, Colloid model of c-s-h and implications to the problem of creep and shrinkage, Materials and Structures 37 (1) (2004) 59–70. doi:10.1007/BF02481627.

[49] A. M. Neville, W. H. Dilger, J. J. Brooks, Creep of plain and structural concrete, Construction Press, 1983.

[50] R. Christensen, Theory of viscoelasticity: an introduction, Elsevier, 1982.

[51] Z. P. Bažant, Y.-P. Xi, S. Baweja, I. Carol, Preliminary guidelines and recommendation for characterizing creep and shrinkage in structural design codes, in: RILEM Proceedings, Chapmann & Hall, 1993, pp. 805–805.

[52] M. Vandamme, F.-J. Ulm, Nanogranular origin of concrete creep, Proceedings of the National Academy of Sciences 106 (26) (2009) 10552–10557.

[53] Q. Zhang, Creep properties of cementitious materials: effect of water and microstructure: An approach by microindentation, Ph.D. thesis, Université Paris-Est (2014).

[54] O. Coussy, Mechanics and Physics of Porous Solids, John Wiley & Sons, 2011.

[55] P. K. Mehta, P. J. Monteiro, Concrete: Microstructure, Properties, and Materials, 3rd Edition, McGraw-Hill New York, 2006.

[56] R. Le Roy, F. Le Maou, J.-M. Torrenti, Long term basic creep behavior of high performance concrete: data and modelling, Materials and structures 50 (1) (2017) 85. doi:10.1617/s11527-016-0948-8.

[57] J.-M. Torrenti, R. Le Roy, Analysis of some basic creep tests on concrete and their implications for modeling, Structural Concrete 19 (2) (2018) 483–488. doi:10.1002/suco.201600197.

[58] Z. P. Bažant, G.-H. Li, Comprehensive database on concrete creep and shrinkage, ACI Materials Journal 105 (6) (2008) 635–637.

[59] M. Vandamme, F.-J. Ulm, Nanoindentation investigation of creep properties of calcium silicate hydrates, Cement and Concrete Research 52 (2013) 38 – 52. doi:http://dx.doi.org/10.1016/j.cemconres.2013.05.006.

[60] J. Frech-Baronet, L. Sorelli, J.-P. Charron, New evidences on the effect of the internal relative humidity on the creep and relaxation behaviour of a cement paste by micro-indentation techniques, Cement and Concrete Research 91 (2017) 39–51.

[61] A. Aili, M. Vandamme, J.-M. Torrenti, B. Masson, J. Sanahuja, Time evolutions of non-aging viscoelastic poisson's ratio of concrete and implications for creep of c-s-h, Cement and Concrete Research 90 (2016) 144 – 161. doi:http://dx.doi.org/10.1016/j.cemconres.2016.09.014.

[62] A. Aili, M. Vandamme, J.-M. Torrenti, B. Masson, Theoretical and practical differences between creep and relaxation poisson's ratios in

linear viscoelasticity, Mechanics of Time-Dependent Materials 19 (4) (2015) 537–555. doi:10.1007/s11043-015-9277-5.

[63] Z. Bažant, A. Asghari, J. Schmidt, Experimental study of creep of hardened portland cement paste at variable water content, Materials and Structures 9 (4) (1976) 279–290.

[64] G. Abiar, Cinétique de dessiccation et déformations différées du béton (analyse et modélisation), Ph.D. thesis, École Nationale des Ponts et Chaussées (1986).

[65] H. Köhler, The nucleus in and the growth of hygroscopic droplets, Transactions of the Faraday Society 32 (1936) 1152–1161.

[66] H. Chen, M. Wyrzykowski, K. Scrivener, P. Lura, Prediction of self-desiccation in low water-to-cement ratio pastes based on pore structure evolution, Cement and concrete research 49 (2013) 38–47.

[67] Z. Hu, Prediction of autogenous shrinkage in fly ash blended cement systems, Ph.D. thesis, École Polytechnique Fédérale de Lausanne (2017).

[68] J. Walraven, J. Shen, On the applicability of the superposition principle in concrete creep, Mechanics of Creep Brittle Materials 2 (1991) 282–295.

[69] J.-M. Torrenti, A. Aili, Modelling of the long term behaviour of prestressed concrete structures: the case of nuclear power plants, in: Proceedings of 5th International fib Congress, Melbourne, Australia, October 2018.

[70] O. Bernard, F.-J. Ulm, E. Lemarchand, A multiscale micromechanics-hydration model for the early-age elastic properties of cement-based materials, Cement and Concrete Research 33 (9) (2003) 1293 – 1309. doi:http://dx.doi.org/10.1016/S0008-8846(03)00039-5.

[71] G. Constantinides, F.-J. Ulm, The effect of two types of c-s-h on the elasticity of cement-based materials: Results from nanoindentation and micromechanical modeling, Cement and concrete research 34 (1) (2004) 67–80.

[72] J. Sanahuja, L. Dormieux, G. Chanvillard, Modelling elasticity of a hydrating cement paste, Cement and Concrete Research 37 (10) (2007) 1427 – 1439. doi:http://dx.doi.org/10.1016/j.cemconres.2007.07.003.

[73] C. Pichler, R. Lackner, H. A. Mang, A multiscale micromechanics model for the autogenous-shrinkage deformation of early-age cement-based materials, Engineering fracture mechanics 74 (1) (2007) 34–58.

[74] S. Ghabezloo, Association of macroscopic laboratory testing and micromechanics modelling for the evaluation of the poroelastic parameters of a hardened cement paste, Cement and Concrete Research 40 (8) (2010) 1197–1210.

[75] B. Pichler, C. Hellmich, Upscaling quasi-brittle strength of cement paste and mortar: A multi-scale engineering mechanics model, Cement and Concrete Research 41 (5) (2011) 467 – 476. doi:http://dx.doi.org/10.1016/j.cemconres.2011.01.010.

[76] T. C. Powers, T. L. Brownyard, Studies of the hardened paste by means of specific-volume measurements, Portland Cement Association Bulletin (1947) 669–712.

[77] H. F. Taylor, Cement Chemistry, Thomas Telford, 1997.

[78] P. Acker, et al., Micromechanical analysis of creep and shrinkage mechanisms, Creep, Shrinkage and Durability Mechanics of Concrete and other quasi-brittle Materials, proceedings of the sixth international conference CONCREEP, Cambridge, MA (2001) 15–25.

[79] C.-J. Haecker, E. Garboczi, J. Bullard, R. Bohn, Z. Sun, S. P. Shah, T. Voigt, Modeling the linear elastic properties of portland cement paste, Cement and Concrete Research 35 (10) (2005) 1948–1960.

[80] A. Boumiz, C. Vernet, F. C. Tenoudji, Mechanical properties of cement pastes and mortars at early ages: Evolution with time and degree of hydration, Advanced cement based materials 3 (3-4) (1996) 94–106.

[81] M. Wyrzykowski, P. Lura, The effect of external load on internal relative humidity in concrete, Cement and concrete research 65 (2014) 58–63.

[82] F. Bourgeois, N. Burlion, J.-F. Shao, Modelling of elastoplastic damage in concrete due to desiccation shrinkage, International journal for numerical and analytical methods in geomechanics 26 (8) (2002) 759–774.

[83] M. T. Van Genuchten, A closed-form equation for predicting the hydraulic conductivity of unsaturated soils, Soil Science Society of America Journal 44 (5) (1980) 892–898.

[84] Y. Xi, Z. P. Bažant, H. M. Jennings, Moisture diffusion in cementitious materials adsorption isotherms, Advanced Cement Based Materials 1 (6) (1994) 248–257.

[85] S. Poyet, Experimental investigation of the effect of temperature on the first desorption isotherm of concrete, Cement and Concrete Research 39 (11) (2009) 1052 – 1059. doi:https://doi.org/10.1016/j.cemconres.2009.06.019.

[86] F. Brue, C. A. Davy, F. Skoczylas, N. Burlion, X. Bourbon, Effect of temperature on the water retention properties of two high performance concretes, Cement and Concrete Research 42 (2) (2012) 384 – 396. doi:https://doi.org/10.1016/j.cemconres.2011.11.005.

[87] M. Wu, B. Johannesson, M. Geiker, A study of the water vapor sorption isotherms of hardened cement pastes: Possible pore structure changes at low relative humidity and the impact of temperature on isotherms, Cement and Concrete Research 56 (2014) 97 – 105. doi:https://doi.org/10.1016/j.cemconres.2013.11.008.

[88] I. Maruyama, G. Igarashi, Numerical approach towards aging management of concrete structures: Material strength evaluation in a massive concrete structure under one-sided heating, Journal of Advanced Concrete Technology 13 (11) (2015) 500–527.

[89] M. Auroy, S. Poyet, P. L. Bescop, J.-M. Torrenti, T. Charpentier, M. Moskura, X. Bourbon, Impact of carbonation on unsaturated water transport properties of cement-based materials, Cement and Concrete Research 74 (2015) 44 – 58. doi:https://doi.org/10.1016/j.cemconres.2015.04.002.

[90] J. M. de Burgh, S. J. Foster, H. R. Valipour, Prediction of water vapour sorption isotherms and microstructure of hardened portland cement pastes, Cement and Concrete Research 81 (2016) 134–150.

[91] L. Charpin, J.-P. Mathieu, T. Sow, Stress concentrations induced by active and passive reinforcements in a concrete containment building, in: Congrès français de mécanique, AFM, Association Française de Mécanique, 2017.

[92] F. Benboudjema, J.-M. Torrenti, Modelling desiccation shrinkage of large structures, in: EPJ Web of Conferences, Vol. 56, EDP Sciences, 2013, p. 02001.

[93] J. Mathieu, L. Charpin, P. Sémété, C. Toulemonde, G. Boulant, J. Haelewyn, F. Hamon, S. Michel-Ponnelle, J. Hénault, F. Taillade, Temperature and humidity-driven ageing of the vercors mock-up, in: Computational Modelling of Concrete Structures: Proceedings of the Conference on Computational Modelling of Concrete and Concrete Structures (EURO-C 2018), February 26-March 1, 2018, Bad Hofgastein, Austria, CRC Press, 2018, p. 215.

[94] Z. P. Bažant, S. T. Wu, Dirichlet series creep function for aging concrete., ASCE J Eng Mech Div 99 (EM2) (1973) 367–387.

[95] R. Sinko, Z. P. Bažant, S. Keten, A nanoscale perspective on the effects of transverse microprestress on drying creep of nanoporous solids, Proceedings of the Royal Society A: Mathematical, Physical and Engineering Sciences 474 (2209) (2018) 20170570. doi:10.1098/rspa.2017.0570.